Paracetamol-Galactose Conjugate: A Novel Prodrug for an Old Analgesic Drug

Article

Paracetamol-Galactose Conjugate: A Novel Pro-drug for an Old Analgesic Drug.

Dr. Federica Sodano, Loretta Lazzarato, Barbara Rolando, Francesca Spyrakis, Carmen De Caro, Salvatore Magliocca, Domenica Marabello, Konstantin Chegaev, Elena Gazzano, Chiara Riganti, Antonio Calignano, Roberto Russo, and Maria Grazia Rimoli

Mol. Pharmaceutics, **Just Accepted Manuscript** • DOI: 10.1021/acs.molpharmaceut.9b00508 • Publication Date (Web): 29 Aug 2019

Paracetamol-Galactose Conjugate: A Novel Pro-drug for an Old Analgesic Drug.

Federica Sodano,[†,] Loretta Lazzarato,[†] Barbara Rolando,[†] Francesca Spyrakis,[†] Carmen De Caro,[○,‡] Salvatore Magliocca,[◊] Domenica Marabello,[#,Δ] Konstantin Chegaev,[†] Elena Gazzano,[^] Chiara Riganti,[^] Antonio Calignano,[‡] Roberto Russo,[‡] Maria Grazia Rimoli.[‡]

[†]Department of Drug Science and Technology, University of Turin, 10125, Turin, Italy;

[○]Department of Science of Health, School of Medicine and Surgery, "Magna Graecia" University of Catanzaro, 88100 Catanzaro, Italy;

[‡]Department of Pharmacy, “Federico II” University of Naples, 80131 Naples, Italy;

[◊]Department of Pharmaceutical and Pharmacological Sciences, University of Padova, 35131 Padova, Italy;

[#]Department of Chemistry, University of Turin, 10125 Turin, Italy;

[Δ]Interdepartmental Center for Crystallography (CrisDi), 10125 Turin, Italy;

[^]Department of Oncology, University of Turin, 10126 Turin, Italy.

TABLE OF CONTENTS (TOC) GRAPHIC

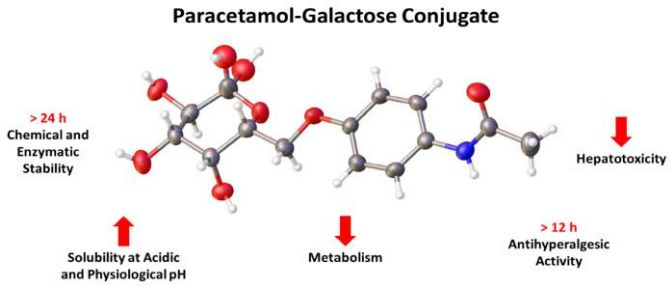

ABSTRACT

Paracetamol has been one of the most commonly used and prescribed analgesic drugs for more than a hundred years. Despite being generally well tolerated, it can result in high liver toxicity when administered in specific conditions, such as overdose, or in vulnerable individuals. We have synthesised and characterised a Paracetamol galactosylated pro-drug (PARgal) with the aim of improving both the pharmacodynamic and pharmacological profile of Paracetamol. PARgal shows a range of physicochemical properties, solubility, lipophilicity and chemical stability at differing physiological pH values and in human serum. PARgal could still be preclinically detected 2 hours after administration, meaning that it displays reduced hepatic metabolism compared to Paracetamol. In overdose conditions, PARgal has not shown any cytotoxic effect in *in-vitro* analyses performed on human liver cells. Furthermore, when tested in an animal pain model, PARgal demonstrated a sustained analgesic effect up to the 12th hour after oral administration. These findings support the use of galactose as a suitable carrier in the development of pro-drugs for analgesic treatment.

Keywords: Paracetamol; Pro-drug; X-ray diffraction; Hepatotoxicity; Metabolism; Hyperalgesia

INTRODUCTION

In 1959, Harper coined the term "latentiation" to describe a chemical modification to a drug that is able to regenerate the parent active substance upon metabolism.[1] Since then, pro-drugs have played a central role in discovery and design, allowing several difficulties in drug development programs to be overcome.[2] Low solubility, premature degradation, short half-life and other pharmacokinetic and pharmacodynamic aspects can, for instance, be tackled with a pro-drug approach.[3] To become a pro-drug candidate, a molecule must present certain features, such as biological inactivity, absence of toxicity, a simple synthetic route, a biolabile drug-carrier conjugate, and ensure the effective concentration of the drug in target tissues.[4]

Paracetamol or acetaminophen, chemically known as *N*-(4-hydroxyphenyl)acetamide, is an over-the-counter analgesic and antipyretic. It is commonly used for fever relief, headaches and other minor aches and pains. It is a major ingredient in numerous cold and flu remedies. In combination with nonsteroidal anti-inflammatory drugs (NSAIDs) and opioid analgesics, Paracetamol is also used in the management of more severe pain (such as postoperative pain) and is one of the most commonly used drugs against hyperalgesia. Together with allodynia, hyperalgesia is one of the two prominent symptoms of the neuropathic pain condition. Some studies have shown that Paracetamol prevents hyperalgesia in several models of nociception.[5-7] Recent works have reported that, when systemically administered, it blocks thermal hyperalgesia in rat plantar incision models,[8] which mimicked painful conditions after surgery or peripheral nerve lesion.[9-10] In addition, Paracetamol is usually the first drug to be used as a remedy in minor illnesses in children. Taken in therapeutic doses, Paracetamol is remarkably well tolerated and metabolised, and the metabolic products are excreted in the urine. In overdose or in vulnerable individuals, however, this drug is responsible for high liver toxicity. In the past 40 years, the metabolism of Paracetamol has been the subject of several studies.[11-13] As shown in Scheme 1, it is principally metabolised to non-toxic sulfate (Paracetamol-Sul) and glucuronide (Paracetamol-Gluc) derivatives, but a variable amount is also metabolised by the cytochrome P-450 system (primarily CYP 2E1) to *N*-acetyl-*p*-benzoquinone imine (NAPQI), *via* an oxidation process, or to 4-aminophenol, *via* a de-acylation mechanism.[11-13] Both derivatives are toxic, with the first being particularly so. As they are unstable, NAPQI and 4-aminophenol bind to essential cellular macromolecules, leading to cell death if not promptly retrieved by a glutathione scavenging process.

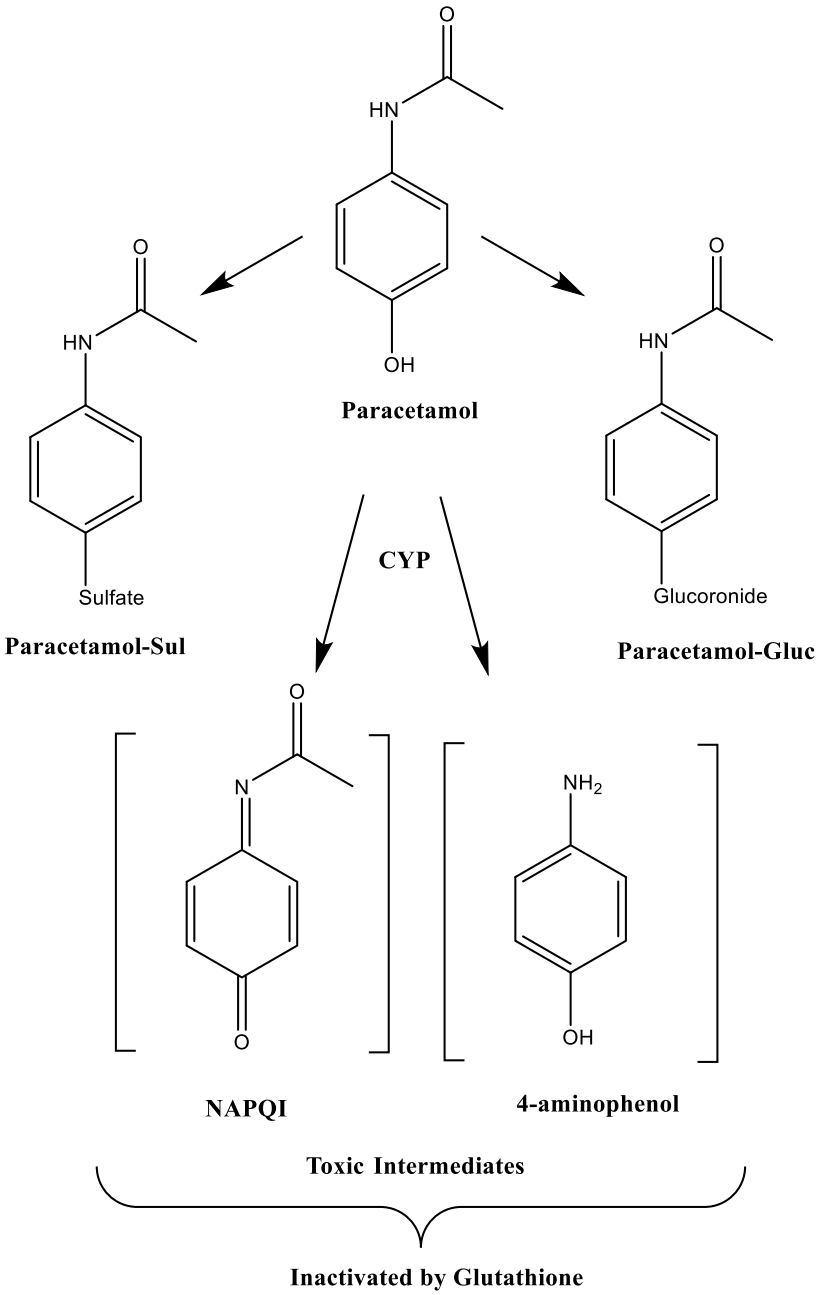

Scheme 1. Metabolism of Paracetamol

In the case of overdose, and when the normal balance of detoxification is upset by the up-regulation of the P450 system or by fasting, and when the glutathione-scavenging system is depleted, toxic metabolites bind to cell structures causing centrilobular necrosis of the liver.[11-13] The risk of overdose and irreversible hepatic damage could be even higher, as Paracetamol is not subject to medical prescription. Additionally, the pharmacological effect lasts between 2 and 4 hours as much of the orally-administered Paracetamol is cleared from the body before reaching peak plasma concentration, due to strong phase-one metabolism.[14-15]

In order to overcome these drawbacks, a water-soluble ester pro-drug (propacetamol) of Paracetamol that is suitable for parenteral administrations has already been marketed in some countries, such as France, but not in others, such as the United States. This is because the pro-drug has a lower local tolerance profile than its parent drug.[16-17] Furthermore, some glycoside pro-drugs of Paracetamol have been developed that display slight improvements to their solubility and pharmacokinetic profiles.[14] There is, thus, the need to design more effective Paracetamol formulations to improve its pharmacokinetic, pharmacodynamic and toxicological properties. With this aim in mind, a galactosylated pro-drug of Paracetamol, *N*-(4-(D-α,β-galactopyranose-6-yl)oxyphenyl)acetamide (PARgal) has been designed, synthesised and reported in this paper. D-galactose has been chosen as a simple and natural carrier because of the results of previous works,[18-21] in which the potential of galactosylated pro-drugs and their chemical stability have been demonstrated,[21] in terms of site specificity,[18] toxicity,[19-20] and solubility.[20-21] In each case, the use of D-galactose generally improved pharmacokinetic and/or pharmacodynamic features and decreased adverse effects.[18-21] In this work, the crystalline structure of PARgal has been determined by X-ray diffraction (XRD), and its physicochemical profile has been analysed, in terms of solubility, lipophilicity and chemical stability at different physiological pH values (7.4 and 1.2), in order to simulate the blood and gastric environments, respectively, and stability in human serum (HS) has also been investigated. The difference in water solubility between PARgal and Paracetamol has been investigated further and supported by molecular dynamic (MD) simulations. Furthermore, *in-vitro* toxicity and the metabolism of PARgal in human liver cells (HepG2) has been evaluated using Paracetamol as the reference compound. Finally, the antihyperalgesic activity of both compounds has been investigated in an *in-vivo* animal-pain model. The results suggest that PARgal may be a valid alternative to Paracetamol from a physicochemical, pharmacodynamic, toxicological and pharmacological point of view.

EXPERIMENTAL SECTION

Chemistry

Reagents and solvents were purchased from commercial sources (Sigma Aldrich). The compounds were purified by flash chromatography under pressure using Merck silica gel 60. The reactions progress was monitored by thin-layer chromatography (TLC) performed on 0.25 mm silica gel coated aluminium plates (60 Merck F254) using two solutions in a sequential manner: ethanol/10% vanillin and ethanol/20% sulfuric acid as visualising agents. Anhydrous THF was freshly distilled under nitrogen from Na/benzophenone ketyl. NMR spectra for ^{1}H and ^{13}C were recorded at room temperature on a JEOL ECZ-R 600 at 600 MHz and 150 MHz, respectively. Chemical shifts (δ) are

given in parts per million (ppm), relative to $SiMe_4$ and coupling constants (J) in Hertz (Hz). The signal multiplicities are reported as: s = singlet, d = doublet, dd = doublet of doublets, m = multiplet. ESI spectra were recorded on a Micromass Quattro API micro (Waters Corporation, Milford, MA, USA) mass spectrometer. Data were processed using a Mass-LynxSystem V4.1 SCN 714 (Waters).

The purity of PARgal, the separation and quantitation of Paracetamol and PARgal in stability and solubility assessments were performed by HPLC analyses. HPLC instrument: HP 1100 chromatograph system (Agilent Technologies, Palo Alto, CA, USA) equipped with a quaternary pump (model G1311A), a membrane degasser (G1379A) and a diode-array detector (DAD) (model G1315B) integrated into the HP1100 system. Data analyses were processed using HP ChemStation system (Agilent Technologies). HPLC conditions: EC Nucleosil 100-5 C18 HD column (250×4.6mm, 5 µm; Macherey-Nagel); CH_3CN 0.1% TFA/H_2O 0.1% TFA 90/10 v/v as eluent; flow rate = 1.0 mL min^{-1}; injection volume = 20 µL (Rheodyne, Cotati, CA). The column effluent was monitored at 226, 245 and 254 nm (referenced against an 800 nm wavelength) for the purity analysis while at 245 nm for the quantitation of the compounds in stability and solubility assessments. The calibration curves obtained by analysing standard solutions, in a concentration range of 1-100 µM, allowed to quantify the compounds ($r^2 > 0.99$). All analytical samples were filtered by 0.45 µm PTFE filters (Alltech).

Synthesis of N-(4-(1,2,3,4-di-O-isopropylidene-D-α-galactopyranose-6-yl)-oxyphenyl)acetamide (PARgalket)

DIAD (1.35 mL, 6.87 mmol) was added at 0°C to a solution of PPh_3 (1.80 g, 6.87 mmol) in dry THF (20 mL) and stirred under positive N_2 pressure. The reaction mixture was stirred until an abundant white precipitate formed. Paracetamol (1.00 g, 6.62 mmol) was added in one portion, followed, after 15 minutes, by a solution of 1,2,3,4-di-*O*-isopropylidene-D-α-galactopyranose (1.72 g, 6.62 mmol) in dry THF (20 mL). The resulting solution was heated at reflux overnight. The next day, the reaction mixture was concentrated via rotary evaporation, diluted with Et_2O (100 mL) and the organic solvent was washed with NaOH 1M (3 × 50 mL), and brine. It was then dried and evaporated under reduced pressure. The residue was partially purified by flash chromatography using Petroleum Ether/EtOAc (80/20, v/v) as the eluent. The white solid was further purified by flash chromatography using Petroleum Ether/*i*-PrOH (9/1, v/v) to give PARgalket as a white foamy solid. (1.44 g, Yield 55%). ^{1}H NMR (600 MHz, $CDCl_3$, Figure S1) δ 1.34 (s, 3H, CH_3), 1.35 (s, 3H, CH_3), 1.46 (s, 3H, CH_3), 1.51 (s, 3H, CH_3), 2.13 (s, 3H, COCH_3), 4.09 – 4.17 (m, 3H, CH_2 and C*H*), 4.34 – 4.36 (m, 2H, 2C*H*), 4.65 (dd, J^1_{HH} = 2.75 Hz, J^3_{HH} = 8.03 Hz, 1H, C*H*), 5.57 (d, J^3_{HH} = 4.82 Hz, 1H, C*H*), 6.86 (d, *J* = 9.0 Hz, 2H, 2CH_{Ar}), 7.37 – 7.39 (m, 2H, 2CH_{Ar}), 7.51 (s, 1H, N*H*). ^{13}C NMR (150 MHz, $CDCl_3$) δ ppm:

24.2, 24.4, 24.9, 25.9, 26.0, 26.1, 66.1, 66.9, 70.5, 70.9, 96.3, 108.7, 109.4, 115.0, 121.7, 131.2, 155.3, 168.3. ESI-MS $[M+Na]^+$: m/z 416.2.

Synthesis of N-(4-(D-α,β-galactopyranose-6-yl)-oxyphenyl)acetamide (PARgal)

A solution of PARgalket (1.24 g, 3.15 mmol) in TFA/water (90/10, v/v, 10 mL), was stirred at room temperature for 15 min. The solvent was removed under reduced pressure; the residue was dissolved in toluene (40 mL) and concentrated again *via* rotary evaporation for three times. Finally, the obtained rubber-like compound was treated with a small amount of cold MeOH to give a white powder. The solid was filtered, washed with cold MeOH and Et_2O, and then dried. The analytically pure sample was obtained *via* crystallisation from an EtOH / H_2O mixture, (0.890 g, Yield 90%). In NMR spectra using DMSO-d_6 as the solvent,[22] the signals of four anomers, namely α- and β- galactopyranose and α- and β- galactofuranose, were observed. ^{1}H NMR (600 MHz, DMSO-d_6, Figure S2a and b) δ 1.99 (s, 3H, COCH_3), 3.25 – 3.33 & 3.54 -3.62 (m, 2H, CH_2), 3.70 – 4.15 (m, 4H, 4C*H*), 4.30 (d, J^3_{HH} = 8.02 Hz, 0.49 H) 4.93 (d, J^3_{HH} = 3.37 Hz, 0.14 H), 4.97 (d, J^3_{HH} = 3.19 Hz, 0.24 H), 5.00 (d, J^3_{HH} = 4.25 Hz, 0.04 H), (C*H*), 6.82 – 6.86 (m, 2H, 2CH_{Ar}), 7.45 – 7.47 (m, 2H, 2CH_{Ar}), 9.78 (s, 1H, N*H*). ^{13}C NMR (150 MHz, DMSO-d_6) δ 23.9, 67.6, 68.0, 68.1, 68.3, 68.5, 68.6, 68.8, 69.2, 69.4, 69.5, 71.9, 72.6, 73.2, 75.8, 77.4, 81.2, 81.7, 82.6, 92.8, 97.4, 101.8, 114.4, 120.6, 132.6, 154.3, 167.9. However, in NMR spectra using D_2O as the solvent, the signals of only three anomers were observed. ^{1}H NMR (600 MHz, D_2O, Figure S3) δ 2.15 (s, 3H, COCH_3), 3.53 (m, 0.64H, α-galactopyranose anomer), 3.68 (dd, J^1_{HH} =10.09 Hz, J^3_{HH} = 2.75 Hz, 0.64 H, α-galactopyranose anomer), 3.84 (dd, J^1_{HH} =10.32 Hz, J^3_{HH} = 3.67 Hz, 0.33 H, α-galactopyranose anomer), 3.89 (dd, J^1_{HH} =10.32 Hz, J^3_{HH} = 2.75 Hz, 0.33 H, β-galactopyranose anomer), (CH_2O), 4.03 – 4.09 (m, 1.67 H), 4.18 – 4.25 (m, 1.93 H), 4.39 – 4.41 (m, 0.27 H), (4C*H*), 4.63 (d, J^3_{HH} = 8.02 Hz, 0.47 H, α-galactopyranose anomer), 5.25 (d, J^3_{HH} = 2.29 Hz, 0.05 H, α/β-galactofuranose anomer), 5.30 (d, J^3_{HH} = 3.90 Hz, 0.40 H, β-galactopyranose anomer), (C*H*O), 7.03 – 7.05 (m, 2H, 2CH_{Ar}), 7.32 – 7.34 (m, 2H, 2CH_{Ar}). ESI-MS $[M+Na]^+$: m/z 336.1. HPLC purity ≥ 95% (t_R = 3.72 and 5.49 min, α- and β-galactopyranose anomers, 65% and 35%, respectively, Figure S4). HRMS (ESI) calculated for $C_{14}H_{19}NNaO_7$ $(M+Na)^+$ 336.1054, observed 336.1057.

X-Ray Diffraction

X-ray data were obtained at room temperature using an Oxford Diffraction Gemini R Ultra diffractometer. Both powder patterns and single crystal data were collected with mirror monochromatized Cu-Kα radiation (1.54184 Á).[23] The CrysAlisPro package was used for data collection and integration,[24] SHELXT,[25] SHELXL for refinement and Olex2 for graphics.[26-27] The

compound crystallises in the ortorhombic $P_2 1_2 1_2 1$ space group with Z=4. All but the hydrogen atoms were anisotropically refined. All H atoms were located on difference Fourier maps, but were calculated and refined with U_{iso}=1.2 or 1.5 U_{eq} of the bonded atom. Crystal data: a= 6.4289(3) Å, b= 12.8201(6) Å, c= 17.5882(7) Å, V= 1449.61(11) Å3, Z= 4, 7751 reflections measured, 2216 unique (R_{int} = 0.0575) which were used in all calculations. The final R_1 was 0.0475 ($I > 2\sigma(I)$) and wR_2 was 0.1165 (all data), max/min peak 0.255/-0.222, CCDC 1815135. Further details of the crystal data and refinement are reported in Table S1, S2 and S3.

X-Ray Powder Diffraction

X-Ray Powder Diffraction (XRPD) patterns were obtained at room temperature using an Oxford Diffraction Gemini R Ultra diffractometer, with mirror monochromatised Cu-Kα radiation (λ=1.54184 Å). The powder of each sample was mixed with a little drop of hydrocarbon-based oil to provide a ball of about 0.5 mm and then mounted on a glass capillary.[28] Collection parameters: maximum resolution 1.4 Å, exposure time 30 s and data integration with CrysAlis Pro software.[24]

Molecular Dynamics

PARgal was parametrised with the AM1-BCC charge method, as implemented in the antechamber package.[29] The MD simulations were setup using the BiKi Life Science suite (http://www.bikitech.com) and the MD simulations were run with Gromacs 4.6.1.[30] The TIP3P solvation model was used. The solvated system was first minimised by 5000 steps of steepest descent. Then, three subsequent steps of equilibration were run for 100 ps in NVT ensemble were run at 100 K, 200 K and 300 K. Finally, 1-ns-long NPT simulation was run to reach the pressure equilibrium condition. No restraint was applied. The integration step was set equal to 1 fs. The Verlet cut-off scheme, the Bussi−Parrinello thermostat,[31] LINCS for the constraints (all bonds), and the particle mesh Ewald for electrostatics, with a short-range cutoff of 11 Å, were used. The first production was carried out in the NVT ensemble at 300 K without any restraint for 20 ns. Ten ligand replicas were present in the water box, corresponding to a ligand concentration of about 0.06 M. For the second production, two replicas were run in the NVT ensemble at 300 K for 50 and 35 ns, respectively. Ten ligand replicas were located in a larger water box to reach a ligand concentration similar to the solubility one, that is, 0.016 M.

Stability in SGF, PBS and human serum

A 10 mM solution of PARgal or Paracetamol in DMSO was added to either simulated gastric fluid (SGF- without pepsin, 2.0 g/L sodium chloride and 2.917 g/L HCl, pH 1.2) or PBS (pH 7.4, 50 mM)

(2.3 g of disodium hydrogen orthophosphate, 0.19 g of potassium dihydrogen orthophosphate and 8.0 g of sodium chloride in sufficient water to produce 1000 mL and adjusted pH if necessary). The resulting solutions (100 µM) were maintained at 37 ±0.5°C. 20 µL aliquots were withdrawn at appropriate time intervals and analysed by HPLC. In this case, chemical stability investigations were conducted on a large scale (5 mL), meaning that the aliquots were not replenished. A 10 mM solution of PARgal or Paracetamol in DMSO was added to human serum (from human male AB plasma, USA origin, sterile-filtered, Sigma–Aldrich). The resulting solutions (200 µM) were maintained at 37 °C ±0.5°C. At specific time intervals, 300 µL of each reaction mixture was withdrawn and added to 300 µL of CH_3CN that contained 0.1% TFA in order to deproteinise the serum. Samples were sonicated, vortexed and then centrifuged for 10 minutes at 2150 g. Each clear supernatant was filtered and analysed by HPLC analysis, as reported above. Again, stability investigations in HS were conducted on a large scale (2 mL) and the aliquots were not replenished.

Solubility assessment in SGF, PBS and water

Solubility was assessed in PBS (pH 7.4, 50 mM), SGF-without pepsin (pH 1.2) and deionised water. (20 mg) of the test compounds were added to 5 mL of PBS, SGF and water in glass tubes in triplicate and stirred on a magnetic stirrer for 6 hours at 25°C. The suspensions were filtered, appropriately diluted and the concentration of filtrate was determined by HPLC analysis, as reported above.

Distribution Coefficient

The distribution coefficients of the compounds at pH 1.2 (log $D^{1.2}$) and pH 7.4 (log $D^{7.4}$) in *n*-octanol and either SGF or PBS were experimentally obtained using the shake-flask technique at room temperature as previously described.[21]

Pharmacological studies

Chemicals

Plasticware for cell cultures was provided by Falcon (Becton Dickinson, Franklin Lakes, NJ). Unless otherwise specified, reagents were from Sigma-Aldrich S.r.l. (Milan, Italy).

Cells

Human liver-cancer cells HepG2 (from American Type Culture Collection, ATCC, Manassas, VA) were cultured in Dulbecco's modified Eagle's medium (Gibco, Paisley, UK) supplemented with 10 % fetal bovine serum (FBS), 1% nonessential amino acids (NEAA) and 1% penicillin/streptomycin. Cells were maintained in a humidified atmosphere at 37 °C and 5% CO_2.

Measurement of extracellular lactate dehydrogenase (LDH) activity

The cytotoxic effect of the drugs was measured as the leakage of LDH activity into the extracellular medium using a Synergy HT microplate reader (BioTek Instruments, Winooski, VT), as previously described.[32] Intracellular and extracellular enzyme activities were expressed as μmol of NADH oxidized/min/dish. Extracellular LDH activity was calculated as the percentage of the total (intracellular + extracellular) LDH activity in the dish.

Sample preparation for the qualitative evaluation of metabolites

In order to qualitatively evaluate the drug metabolites, HepG2 cells were incubated with either 100 μM Paracetamol or 100 μM PARgal. After 2 hours of incubation, cells were washed with PBS, collected and lysed in 0.3 mL of ice-cold RIPA buffer (50 mM Tris, 10 mM EDTA, 1% v/v Triton-X100; pH 7.5). Lysates were clarified by centrifugation at 15,000 g for 10 minutes and the pellets were discarded. The supernatants were transferred into fresh tubes for UPLC-MS analysis. Each experimental point was performed in triplicate.

UPLC-MS analysis

The qualitative evaluation of PARgal and Paracetamol metabolites was carried out on an Acquity Ultra Performance LC™, Waters Corporation Milford MA, USA, equipped with BSM, SM, CM and PDA detectors. UPLC conditions: Aquasil C18 column (200×4.6 mm, 5 μm); CH_3CN 0.1% HCOOH / H_2O 0.1% HCOOH 10/90 v/v as mobile phase; flow rate = 0.5 mL min^{-1}; Micromass Quattro microTM API Esci multi-mode ionisation as detector. For PARgal, the molecular ion $[M+H]^+$ was used for the qualitative measurements of the analyte: m/z: 314. MS conditions: drying gas (nitrogen) heated at 350 °C; flow rate = 800 L/h; nebuliser gas (nitrogen) at 80 L/h; capillary voltage in negative mode at 3000 V; fragmentor voltage at 30 V. For Paracetamol and the metabolites, the molecular ion $[M-H]^-$ was used for the evaluation: Paracetamol m/z: 150; Paracetamol-Glucoronide (Paracetamol-Gluc) m/z: 302; Paracetamol-Sulphate (Paracetamol-Sul) m/z: 230; Paracetamol-Glutathione (Paracetamol-Glut) m/z: 456. Chromatogram examples of Paracetamol and PARgal metabolites are reported in Figure S5 and S6, respectively.

Animal model

Ten-week-old male Swiss CD1 mice weighing 30–35 g were purchased from Charles Rivers (Calco, Italy). They were kept for 1 week under controlled environmental conditions (22 ± 1°C, 12:12 h light/dark cycle), with *ad libitum* access to water and a standard rodent chow diet. All procedures

involving the mice were carried out in accordance with Institutional Guidelines, and complied with the Italian Ministry of Health and the associated guidelines of the European Communities Council Directive. The procedures reported here were approved by the Institutional Committee on the Ethics of Animal Experiments (CSV) at the University of Naples "Federico II" and by the Ministry of Health under protocol no. 2014-0084607. At the end of the experiments, the animals were euthanised by CO_2 overdose.

Post-operative pain model: paw incision

All mice were anesthetised with an enflurane/O_2 mixture which was maintained using a mask during the administration procedure. The left paw was disinfected with betadine; a 1 cm longitudinal incision was made with a number 12 blade through the skin and fascia of the plantar aspect of the foot, starting 0.5 cm from the proximal edge of the heel and extending toward the toes. In most animals, the plantaris muscle was elevated and incised longitudinally. The wound was closed with a 5-0 nylon thread. After surgery, the animals were allowed to recover in their cages. The incisions were checked daily, and any signs of wound infection or dehiscence meant that the animal was excluded from the study. The Paracetamol doses (200 mg/kg/os) and equimolecular doses of PARgal (438 mg/kg/os) were administrated 10 minutes after paw incision.

Mechanical hyperalgesia

Mechanical hyperalgesia was evaluated using Randall-Selitto apparatus for mice (Ugo Basile, Varese, Italy). The paw-withdrawal threshold (g) was measured to a calibrated pressure. Hyperalgesia was assessed on both ispsilateral (incision) and contralateral (not incision) paws before (basal), as well as 1, 2, 4, 7,10, 24 and 48 h after oral administration. Each paw was tested twice per session. The cut-off force was set at 120 g.

Statistical analysis

All analyses were performed using GraphPad Software Inc., Version 7.0, San Diego, CA. The statistical significance was determined using the Student's t test or by one- or two-way analyses of variance (ANOVA) followed by a Bonferroni's *post-hoc* test for multiple comparisons

RESULTS and DISCUSSION

Synthesis

The synthesis of PARgal was performed in two steps. First, the Paracetamol residue was introduced onto the 6-carbon atom of 1,2,3,4-di-*O*-isopropylidene-D-α-galactopyranose, using Mitsunobu conditions. Subsequently, the complete deprotection of the ketals under acidic conditions (90%

trifluoroacetic acid, TFA) gave the 6-substituted galactose, PARgal (Scheme 2).[20] The targeted pro-drug was obtained as a white, highly crystalline powder and characterised by XRPD (Figure 3).

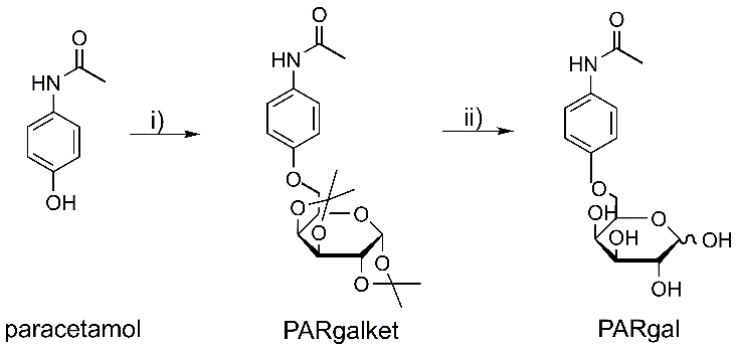

Scheme 2. Synthesis of PARgal. Reaction conditions: i) PPh_3, DIAD, Paracetamol, THF, reflux; yield 55%. ii) 90% CF_3COOH, rt; yield 90%.

X-ray diffraction

The crystallisation behaviour of PARgal was investigated in DMSO and water. Two polymorphic forms were found, one deriving from the slow evaporation of a dimethylsulfoxide (DMSO) solution, and the other from crystallisation in water. The powder pattern of the DMSO polymorph (Figure 1) was characterised by main peaks at 2Θ values of 8.47°, 10.05°, 13.75°, 14.63°, 16.74°, 18.33°, 20.26°, 21.49°, 24.84°, 25.72°, 29.77°, 32.76°, 36.63° and 38.39°, while the water polymorph (Figure 1) by main peaks at 2Θ values of 8.47°, 11.11°, 14.63°, 16.57°, 18.85°, 20.97°, 22.20°, 22.90°, 24.13°, 26.24°, 26.94°, 30.13° and 33.64°. The crystals obtained from DMSO were submitted to single crystal X-ray diffraction (XRD). The obtained molecular structure is reported in Figure 2, while details on crystal data, molecular bond lengths and angles are in Table S1-S3. According to X-ray analyses, one whole molecule is present in the asymmetric unit of PARgal. The O11-H11 group is located in two different positions with relative occupancy of 0.65 and 0.35, which correspond to α- and β-galactopyranose. The 65/35 ratio of the anomeric mixture is in accordance with the findings of the HPLC purity analyses (Figure S4).

The exact structure of PARgal, as obtained by XRD on DMSO crystals (Figure 3, red line), was then compared with the patterns collected for the powder that was directly obtained from the synthesis and used for biological studies (Figure 3, black line), and the powder pattern of the DMSO polymorph (blue line). As shown in Figure 3, the correspondence of the three diffractograms demonstrates that a single polymorph was produced by both the synthesis and re-crystallisation in DMSO solution (Figure 3).

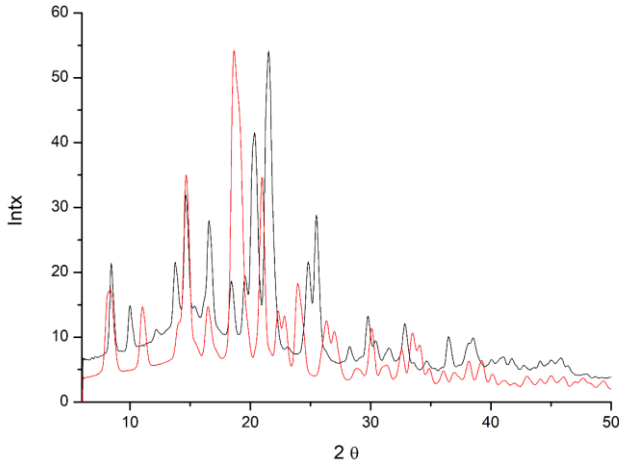

Figure 1. XRPD patterns collected from the two polymorphs of PARgal obtained in DMSO (red line) and water (black line) solutions.

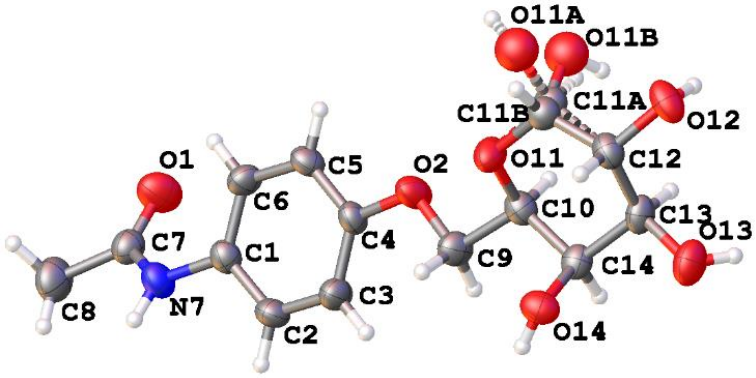

Figure 2. View of the PARgal molecule with thermal ellipsoids (50% probability) and atom labelling.

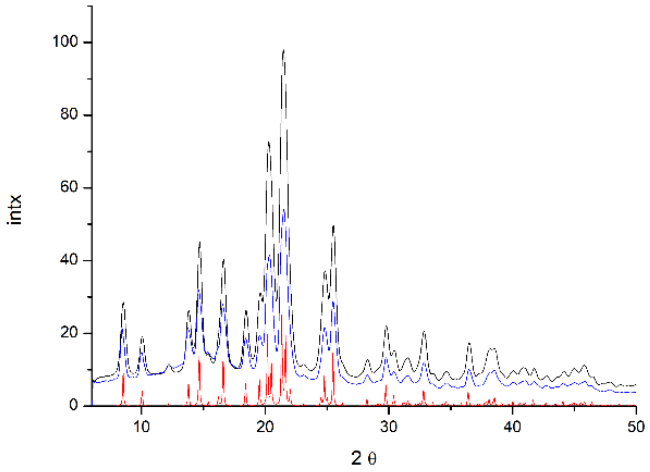

Figure 3. XRPD patterns collected for PARgal, as obtained from the synthesis (black line) and the DMSO solution (blue line), compared with the pattern calculated from the XRD structure (red line).

Physicochemical characterisation

The chemical stability of PARgal and Paracetamol was determined at 37°C and pH 7.4 in phosphate buffered saline (PBS), and at pH 1.2 in simulated gastric fluid (SGF-without pepsin), in order to mimic the blood and gastric environments, respectively. Stability was also evaluated in human serum (HS). PARgal demonstrated better stability, under all the conditions studied, than other galactosylated pro-drugs.[20-21] After 24 hours of incubation, the release of the "active" substance, in our case Paracetamol (Figure S7, first peak, t_R = 4.55 min), from its pro-drug (Figure S7, second peak, t_R = 5.88 min) was lower than 5% and so considered negligible in every used media (Figure S7). Additionally, the distribution coefficients (log D^{pH}) of Paracetamol and PARgal in *n*-octanol-PBS (pH 7.4) and in *n*-octanol-SGF (pH 1.2) were measured. Both coefficients were independent of pH, reflecting the absence of ionisable groups. Only the experimental values in *n*-octanol-PBS are reported in Table 1. According to data reported in the literature,[33] the value of the experimental coefficient distribution for Paracetamol is 0.43, while that measured for PARgal was -1.65. PARgal was found to be much more hydrophilic, which is the result of increasing the number of hydroxyl groups via the conjugation of Paracetamol to the sugar component.

The solubilities of the pro-drug and its parent drug were evaluated in the same media used for the chemical stability analysis (pH 7.4 in PBS and pH 1.2 in SGF-without pepsin) and in water at 25 °C. In both buffered solutions (PBS and SGF-without pepsin), PARgal was found to be slightly more soluble than Paracetamol, which is in accordance with the decrease in lipophilicity. Furthermore, because of the absence of ionisable groups, the solubility of PARgal in water was not dependent on pH and was quite similar to the value found in SGF and PBS solutions, but surprisingly lower than that of Paracetamol. In contrast to other galactosylated pro-drugs,[20-21] the solubility of PARgal in water was about three times lower than that of Paracetamol. This finding led us to study the behaviour of the molecule in water.

	Lipophilicity [a]	Solubility (mg/mL) [a]		
Compounds	log $D^{7.4}$	SGF	PBS	Water
PARgal	-1.65 ±0.09	5.1 ±0.3	5.0 ±0.1	4.0±0.2
Paracetamol	0.43 ±0.04	3.4 ±0.1	3.5 ±0.20	14.0 ±0.3

Table 1. Physicochemical characterisation of PARgal and Paracetamol: lipophilicity (log D^{pH}) and solubility at 25 °C. [a] Results are expressed as mean values ± SD.

MD simulations

To understand the decreased solubility in water, MD simulations were carried out on the single molecule and on a set of ten PARgal copies in water solution. The simulations were performed with Gromacs 4.6.1., as implemented in the BiKi Life Science software suite (http://www.bikitech.com). The ligand coordinates obtained by XDR were used as the starting structure. When a single PARgal molecule was simulated, the galactose rings occasionally bended towards the Paracetamol benzene ring, but no intramolecular hydrogen bond was formed within the molecule. When the concentration of the molecule in the solvation box was increased to the solubility concentration (about 0.016 M) and higher (about 0.06 M), PARgal formed aggregates during the simulations. In particular, aggregates of two, three, four, and even five or six molecules were detected, as represented in Figure 4. The aggregates are stabilised by the formation of a number of hydrogen bonds between the galactose moiety and the polar atoms of the Paracetamol region. A few hydrophobic interactions further stabilise the cluster formation. This easy molecular aggregation might explain the molecule's poor solubility in water, regardless of the general polar character of the molecule (Table 1).

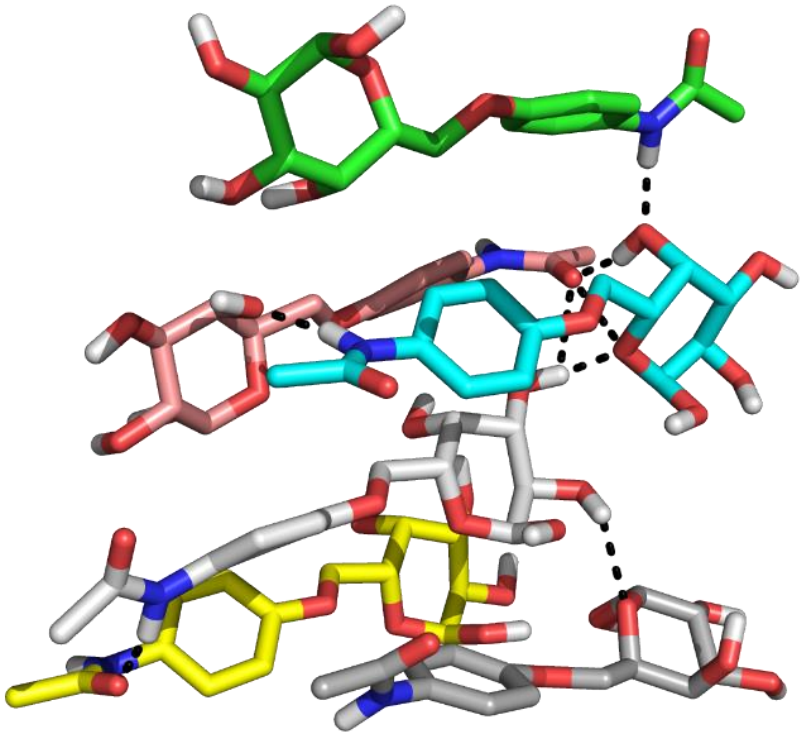

Figure 4. Example of PARgal aggregation during MD simulations. The different PARgal copies are represented as capped sticks and coloured green, rose, cyan, light grey, yellow and dark grey. Hydrogen bonds are shown as black dash lines. The picture was prepared with Pymol v.1.7.6.4.

Toxicological profile of PARgal in human liver cells

In order to evaluate the cytotoxicity of PARgal, with respect to Paracetamol, and obtain preliminary information about their toxicity in the liver, human liver-cancer cells (HepG2) were incubated for 48 hours with different concentrations of the parent and pro-drug.[34-35] The release of LDH, a sensitive index of loss of membrane integrity, was measured. The LDH assay demonstrated that Paracetamol displays significant dose-dependent toxicity at 5 mM concentration, which is in accordance with the data reported in the literature,[36-40] while PARgal reached the same level of toxicity at 10 mM (Figure 5). Interestingly, the pro-drug was non-toxic at 5 mM concentration. In fact, no significant disruption to the membrane integrity of human liver cells was observed at this concentration. At the highest tested concentration (10 mM), PARgal showed a cytotoxic effect that was significantly lower than that of Paracetamol (Figure 5).

According to the literature,[36-42] large doses of Paracetamol cause acute hepatic necrosis as a result of the depletion of glutathione, and of the covalent binding of the reactive metabolites, (4-aminophenol and NAPQI, Scheme 1) to vital cell constituents. In particular, both metabolites initiate an immune response inside liver cells that results in the destruction of the tissues. Moreover, it is generally believed that the presence of a moiety attached to the phenol may minimise the metabolic oxidation rate.[14] Similarly, *O*-derivatives obtained by the conversion of the phenol to a phenyl ether might reduce the formation of toxic bye-products and hepatic damage. The results shown in Figure 5 fully confirm this theory,[14] as the reaction of galactose at Paracetamol *O*-position minimised the hepatotoxicity.

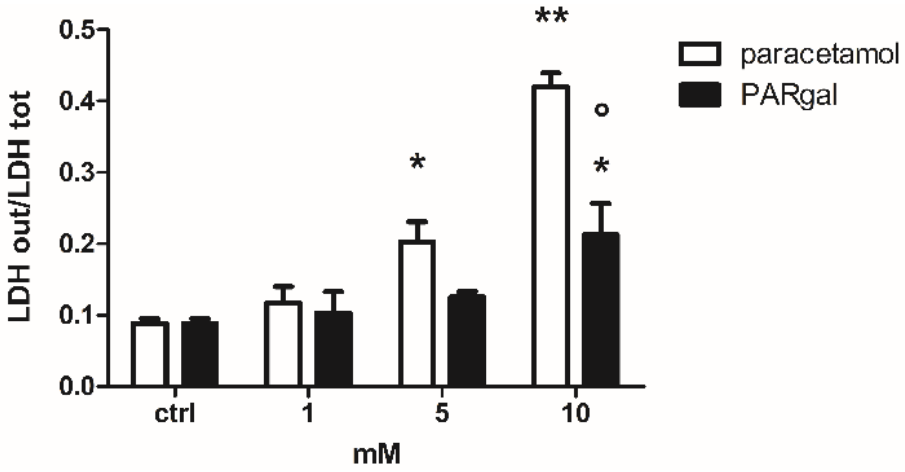

Figure 5. Effect of PARgal and Paracetamol on LDH release into the extracellular medium of HepG2 cells. Cells were incubated for 48 h in either the absence (control) or presence of either 1, 5 and 10 mM Paracetamol or PARgal. Data are presented as means ± SEM (n=3). Vs ctrl: *p<0.05; **p<0.01. Vs Paracetamol 10 mM: °p<0.01.

Evaluation of PARgal and Paracetamol metabolism in human liver cells

To further confirm that the presence of galactose at the *O*-position reduces the toxicity on the hepatic level, the metabolism of PARgal and Paracetamol in liver cells was evaluated in qualitative terms. HepG2 cells were injected with 100 µM solutions of both compounds and evaluated by UPLC-MS after 2 hours. The two non-toxic metabolites, Paracetamol-Gluc and Paracetamol-Sul were the principle species identified, which is in agreement with literature data (see Table 2 and Scheme 1).[11-13] Furthermore, after releasing Paracetamol, the galactosylated pro-drug was metabolised to the Paracetamol-Gluc and Paracetamol-Sul derivatives. The two toxic metabolites, 4-aminophenol and NAPQI were also produced by the metabolism of both Paracetamol and PARgal, but rapidly inactivated by conjugation with reduced glutathione to give the Paracetamol-Glut intermediate (Table 2).

Interestingly, the cells treated with PARgal still displayed some non-metabolised pro-drug after 2 hours of incubation, while those incubated with Paracetamol did not show even a trace of it. Therefore, the stability of PARgal and, at the same time, the slow release of the parent drug, as previously demonstrated, further prove the efficiency of the pro-drug strategy. Hence, the conjugation of the parent drug with galactose led not only to an improvement in the toxicological profile of Paracetamol and a change in its physicochemical properties, in terms of chemical stability, also in human serum, but also a slowing of its metabolic profile.

Compounds	Non-metabolised Drug	Paracetamol	Paracetamol-Gluc	Paracetamol-Sul	Paracetamol-Glut
PARgal	D	ND	D	D	D
Paracetamol	ND	-	D	D	D

Table 2. Detectable (D) and non-detectable (ND) metabolites of PARgal and Paracetamol.

Antihyperalgesic effects of oral Paracetamol and PARgal administration in post-operative pain

The pharmacological efficacy of PARgal and Paracetamol were evaluated in paw-incision-induced hyperalgesia in mice. This hyperalgesia model can be a useful indicator to evaluate both the simple analgesia and clinical efficacy of analgesic drugs against hyperalgesia. Following the incision of the paws, the animals showed signs of hyperalgesia, as compared to basal data (white bar, Figure 6). Single oral treatment with Paracetamol (200 mg/kg/os) produced significant antihyperalgesic activity from the 1st up to the 4th hour, as reported in the literature (Figure 6).[43] PARgal (438 mg/kg/os), administered at an equimolar dose, produced a similar, but prolonged, antihyperalgesic effect. As shown in Figure 6, PARgal analgesic activity was still present at the 12th hour after oral administration. This protracted response was probably due to the slow hydrolysis of Paracetamol from its pro-drug with consequent long-lasting analgesic activity, and could lead to reduced dosing frequency and, consequently, to lower side-effects and overdose risk.

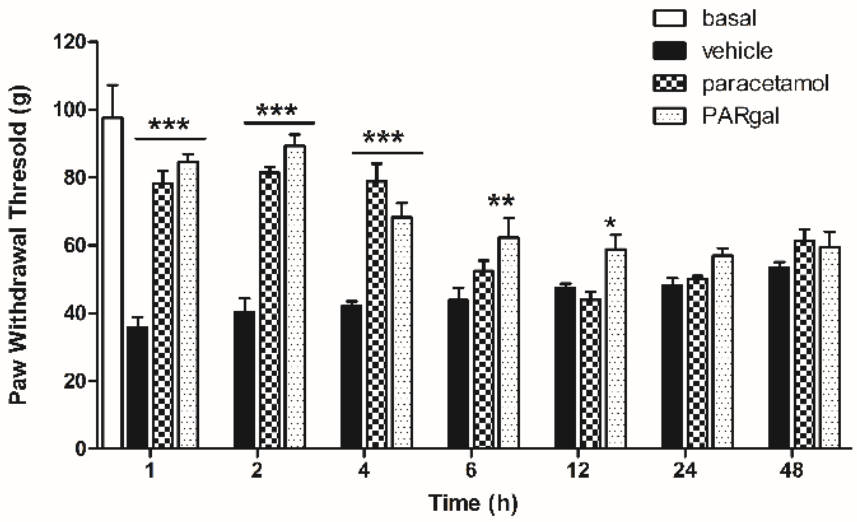

Figure 6. Antihyperalgesic activity of oral PARgal and Paracetamol administration by Randall-Selitto assay. The vehicle (aqueous solution of CMC, 0.5 w/v), Paracetamol (200 mg/kg/os) and PARgal (438 mg/kg/os) were orally administrated 10 minutes before paw incision. Data are expressed as mean ± SEM of six animals for each group. *p<0.05; **p<0.01; ***p<0.001 versus vehicle.

CONCLUSIONS

PARgal, a galactosylated pro-drug of Paracetamol, has been synthesised and characterised with the aim of improving the pharmacodynamic and toxicological profile of Paracetamol. PARgal demonstrated higher stability in human serum, as well as in SGF and PBS media, and reduced metabolism compared with Paracetamol *in-vitro*. Some non-metabolised pro-drug was still present in the liver cells upon two hours from the administration, which was not true for the parent drug. The

slow release of the parent drug led to prolonged analgesic effects, up to the 12th hour, upon oral administration. Furthermore, *in-vitro* hepatotoxicity was drastically lower than that of Paracetamol when PARgal was tested in HepG2 cells in overdose conditions. From a pharmacological point of view, although PARgal showed similar analgesic activity to Paracetamol, it was prolonged over time, both in thermal hyperalgesia,[8] and in a mouse model of mechanical hyperalgesia. This property is particularly appealing in the case of hyperalgesia, which is, often, only a symptom of more serious diseases, such as neuropathic pain.

The obtained results demonstrate that PARgal may be a promising substitute for Paracetamol, and that galactose is a suitable carrier for the development of pro-drugs to be used in analgesic treatment.

ASSOCIATED CONTENT

Supporting Information:

- ^{1}H NMR Spectra of PARgalket (Figure S1);
- ^{1}H NMR Spectra of PARgal in DMSO-d_6 (Figure S2a-b);
- ^{1}H NMR Spectra of PARgal in D_2O (Figure S3);
- Chromatogram of PARgal HPLC purity (Figure S4);
- Crystal data and structure refinement for PARgal (Table S1);
- Bond lengths for PARgal (Table S2);
- Bond angles for PARgal (Table S3);
- Chromatogram example of Paracetamol metabolites (Figure S5);
- Chromatogram example of PARgal metabolites (Figure S6);
- Chromatogram example of Paracetamol Release from PARgal (Figure S7).

AUTHOR INFORMATION

Corresponding Author

* Dr. Federica Sodano, federica.sodano@unito.it; Department of Drug Science and Technology, University of Turin, Via Pietro Giuria 9, 10125 Turin, Italy. Phone: +390116707140; fax number: +390116707162.

Author Contributions

KC and SM synthesised and characterised PARgal. BR evaluated chemical and plasmatic stability, solubility and lipophilicity. DM analysed PARgal structure using XRD and XRPD; FrSp carried out MD simulations; CR and EG performed *in-vitro* experiments; LL analysed the cellular samples by UPLC-MS; CDC and RR performed *in-vivo* experiments; FS conceived and designed the

experiments, analysed data, and wrote the manuscript. FS, AC and MGR contributed to the discussion, review and editing of the manuscript. FS is the guarantor of this work and, as such, had full access to all the data in the study.

Funding Sources

Local funds from the Universities of Turin and Naples supported the research for the present manuscript.

Notes

The authors declare that there are no financial and commercial conflicts of interest.

Abbreviations used:

CYP, cytochrome; DIAD, diisopropyl azodicarboxylate; DMSO, dimethyl sulfoxide; HPLC, high performance liquid chromatography; HS, human serum; LDH, lactate dehydrogenase; MD, molecular dynamics; NAPQI, *N*-acetyl-p-benzoquinone imine; NMR, nuclear magnetic resonance; NSAIDs, nonsteroidal anti-inflammatory drugs; PARgal, *N*-(4-(D-α,β-galactopyranose-6-yl)oxyphenyl)acetamide; PBS, phosphate buffered saline; PPh_3, triphenylphosphine; rt, room temperature; SGF, simulated gastric fluid; TFA, trifluoracetic acid; THF, tetrahydrofuran; UPLC-MS, ultra performance liquid chromatography mass spectrometry; XRD, X-ray diffraction; XRPD, X-ray powder diffraction.

ACKNOWLEDGMENT

We would like to thank Giovanni Esposito and Angelo Russo for animal care and assistance. We also thank the Centro di Competenza sul Calcolo Scientifico (C3S) at the University of Turin (c3s.unito.it) for providing the computational time and resources, and BiKi Technologies for providing the BiKi LiFe Sciences suite. Finally, we thank Dale Lawson for the English language editorial revision.

REFERENCES

(1) Harper, N. J. Drug Latentiation. *J. Med. Pharm. Chem.* **1959**, *1*, 467-500.

(2) Chung, M. C.; Silva, A. T. A.; Castro, L. F.; Güido, R. V. C.; Nassute, J. C.; Ferreira, E. I. Latenciação e formas avançadas de transporte de fármacos. *Rev. Bras. Cienc. Farm.* **2005**, *41*, 155-179.

(3) Testa, B. Prodrug Research: futile or fertile? *Biochem. Pharmacol.* **2004**, *68*, 2097-2106.

(4) Chung, M.-C.; Ferreira, E. I. O processo de latenciação no planejamento de fármacos. *Quim. Nova*, **1999**, *22*, 75-84.

(5) Bianchi, M.; Panerai, A.E. The dose-related effects of Paracetamol on hyperalgesia and nociception in the rat. *Br. J. Pharmacol*. **1996**, 130-132.

(6) Crawley, B.; Saito, O.; Malkmus, S.; Fitzsimmons, B.; Hua, X.Y.; Yaksh, T.L. Acetaminophen prevents hyperalgesia in central pain cascade. *Neurosci. Lett.* **2008**, 50-53.

(7) Toussaint, K.; Yang, X.C.; Zielinski, M.A.; Reigle, K.L.; Sacavage, S.D.; Nagar, S.; Raffa, R.B. What do we (not) know about how Paracetamol (acetaminophen) works? *J. Clin. Pharm. Ther*. **2010**, 617-638.

(8) Girard, P.; Niedergang, B.; Pansart, Y.; Coppé, M.C.; Verleye, M. Systematic evaluation of the nefopam-Paracetamol combination in rodent models of antinociception. *Clin. Exp. Pharmacol. Physiol*. **2011**, 170-178.

(9) Brennan, T.J.; Vandermeulen, E.P.; Gebhart, G.F. Characterization of a rat model of incisional pain. *Pain*, **1996**, 493-501.

(10) Jang, J.H.; Lee, B.H.; Nam, T.S.; Kim, J.W.; Kim, D.W.; Leem, J.W. Peripheral contributions to the mechanical hyperalgesia following a lumbar 5 spinal nerve lesion in rats. *Neuroscience*, **2010**, 221-232.

(11) Bessems, J.G.; Vermeulen, N.P. Paracetamol (acetaminophen)-induced toxicity: molecular and biochemical mechanisms, analogues and protective approaches. *Crit Rev Toxicol.* **2001** *31*, 55–138.

(12) Prescott, L.F. Paracetamol overdosage. Pharmacological considerations and clinical management. *Drugs*, **1983**, *25*, 290–314.

(13) Hodgman, M.J.; Garrard, A.R. A review of acetaminophen poisoning. *Crit Care Clin.* **2012**, *28*, 499–516.

(14) 14. Muhammad, N.; Bley, K.R. Water-soluble acetaminophen analogs. WO 2009/143295 A1, Nov 26, **2019**.

(15) Hardman, J. G.; Limbird, L. E.; Gilman, A. G. Goodman and Gillman's The pharmacological basis of therapeutics 10th ed. McGrawHill, **2001**, pp 704.

(16) Moller, P. L.; Sindet-Pedersen, S.; Petersen, C. T.; Juhl, G. I.; Dillenschneider, A.; Skoglund L. A. Onset of acetaminophen analgesia: comparison of oral and intravenous routes after third molar surgery. *Br. J. Anaesth.* **2005**, *94*, 642–648.

(17) Moller, P. L.; Sindet-Pedersen, S.; Petersen, C. T.; Juhl, G. I.; Dillenschneider, A.; Skoglund L. A. Intravenous acetaminophen (Paracetamol); comparable analgesic efficacy, but better local safety than its prodrug. Propacetamol, for postoperative pain after third molar surgery. *Anesth. Analg*. **2005**, *101*, 90-96.

(18) Perrone, M.G.; Vitale, P.; Ferorelli, S.; Boccarelli, A.; Coluccia, M.; Pannunzio, A.; Campanella, F.; Di Mauro, G.; Bonaccorso, C.; Fortuna, C.G.; Scilimati, A. Effect of mofezolac-galactose distance in conjugates targeting cyclooxygenase (COX)-1 and CNS GLUT-1 carrier. *Eur. J. Med. Chem.* **2017**, *141*, 404-416.

(19) Russo, R.; De Caro, C.; Avallone, B.; Magliocca, S.; Nied-du, M.; Boatto, G.; Troiano, R.; Cuomo, R.; Cirillo, C.; Avagliano, C.; Cristiano, C.; La Rana, G.; Sarnelli, G.; Calignano, A.; Rimoli, M.G. Ketogal: A Derivative Ketorolac Molecule with Minor Ulcerogenic and Renal Toxicity. *Front Pharmacol.* **2017**, *8*, (757), 1-11.

(20) Di Guida, F.; Pirozzi, C.; Magliocca, S.; Santoro, A.; Lama, A.; Russo, R.; Nieddu, M.; Burrai, L.; Boatto, G.; Mollica, M.P.; Sodano, F.; Lazzarato, L.; Chegaev, K.; Meli, R.; Raso, G.M.; Rimo-li, M.G. Galactosylated Pro-Drug of Ursodeoxycholic Acid: Design, Synthesis, Characterization, and Pharmacological Effects in a Rat Model of Estrogen-Induced Cholestasis. *Mol Pharm.* **2018**, 21-30.

(21) Magliocca, S.; De Caro, C.; Lazzarato, L.; Russo, R.; Rolando, B.; Chegaev, K.; Marini, E.; Nieddu, M.; Burrai, L.; Boatto, G.; Cristiano, C.; Marabello, D.; Gazzano, E.; Riganti, C.; Sodano, F.; Rimoli, M.G. Aceclofenac-Galactose Conjugate: Design, Synthesis, Characterization, and Pharmacological and Toxicological Evaluations. *Mol Pharm.* **2018**, 3101-3110.

(22) Mackie, W.; Perli, A.S. Pyranose-furanose and anomeric equilibria influence of solvent and of partial methylation. *Can. J. Chem*, **1966**, *44*, 2039-2049

(23) Enhance Ultra (Cu) X-ray Source, Agilent Technologies

(24) CrysAlisPro, Agilent Technologies, Version 1.171.36.28

(25) Sheldrick, G.M. SHELXT - Integrated space-group and crystal-structure determination. *Acta Cryst.* **2015**, *A71*, 3-8.

(26) Sheldrick, G.M. Crystal structure refinement with SHELXL. *Acta Cryst.* **2015**, *C71*, 3-8.

(27) Dolomanov, O. V.; Bourhis, L. J.; Gildea, R. J., Howard J. A. K., Puschmann H. OLEX2: A Complete Structure Solution, Re-finement and Analysis Program. *J. Appl. Cryst.* **2009**, *42*, 339-341.

(28) Non-drying immersion oil for microscopy, type B, code 1248, Cargille Laboratories

(29) Wang, J.; Wang, W.; Kollman, P. A.; Case, D. A. Automatic atom type and bond type perception in molecular mechanical calculations. *J. Mol. Graph. Model.* **2006**, *25*, 247-260.

(30) Hess, B.; Kutzner, C.; Van Der Spoel, D.; Lindahl, E. Gromacs 4: Algorithms for Highly Efficient, Load-Balanced, and Scalable Molecular Simulation. *J. Chem. Theory Comput.* **2008**, *4*, 435−447.

(31) Bussi, G.; Donadio, D.; Parrinello, M. Canonical Sampling through Velocity Rescaling. *J. Chem. Phys.* **2007**, *126*, 014-101.

(32) Aldieri, E.; Fenoglio, I.; Cesano, F.; Gazzano, E.; Gulino, G.; Scarano, D.; Attanasio, A.; Mazzucco, G.; Ghigo, D.; Fubini, B. The role of iron impurities in the toxic effects exerted by short multiwalled carbon nanotubes (MWCNT) in murine alveolar macro-phages. *Toxicol. Environ. Health Part A* **2013**, *76*, 1056-1071.

(33) Port, A.; Bordas, M.; Enrech, R.; Pascual, R.; Rosés, M.; Ràfols, C.; Subirats, X.; Bosch, E. Critical comparison of shake-flask, potentiometric and chromatographic methods for lipophilicity evaluation (log Po/w) of neutral, acidic, basic, amphoteric, and zwitterionic drugs. *Eur. J. Pharm. Sci.*, **2018**, *122*, 331-340.

(34) Richter, L. H. J.; Beck, A.; Flockerzi, V.; Maurer, H. H.; Meyer, M.R. Cytotoxicity of new psychoactive substances and other drugs of abuse studied in human HepG2 cells using an adopted high content screening assay. *Toxicol Lett.* **2019,** *301*, 79-89.

(35) Roh, T.; De, U.; Lim, S. K.; Kim, M. K.; Choi, S. M.; Lim, D. S.; Yoon, S.; Kacew, S.; Kim, H. S.; Lee, B. M. Detoxifying effect of pyridoxine on acetaminophen-induced hepatotoxicity via suppressing oxidative stress injury. *Food Chem Toxicol.* **2018**, *114*, 11-22.

(36) Manov, I.; Hirsh., M.; Iancu, T.C. N-acetylcysteine does not protect HepG2 cells against acetaminophen-induced apoptosis. *Basic Clin Pharmacol Toxicol*. **2004**, *94*, 213-225.

(37) Shear, N.H.; Malkiewicz, I.M.; Klein, D.; Koren, G.; Randor, S.; Neuman, M.G. Acetaminophen-induced toxicity to human epidermoid cell line A431 and hepatoblastoma cell line HepG2, in vitro, is diminished by silymarin. *Skin Pharmacol*. **1995**, *8*, 279-291.

(38) Nicod, L.; Viollon, C.; Regnier, A.; Jacqueson, A.; Richert, L. Rifampicin and isoniazid increase acetaminophen and isoniazid cytotoxicity in human HepG2 hepatoma cells. *Hum Exp Toxicol.* **1997**, *16*, 28-34.

(39) Bruno, M.K.; Khairallah, E.A.; Cohen, S.D. Inhibition of protein phosphatase activity and changes in protein phosphorylation following acetaminophen exposure in cultured mouse hepatocytes. *Toxicol Appl Pharmacol*. **1998**, *153*, 119-132.

(40) Manov, I.; Hirsh, M.; Iancu, T.C. Ultrastructural features of lymphocyte suppression induced by anthrax lethal toxin and treated with chloroquine. *Exp Toxicol Pathol.* **2002**, *53*, 489-500.

(41) Mitchell, J.R.; Jollow, D.J.; Potter, W.Z.; Davis, D.C.; Gillette, J.R.; Brodie, B.B. Acetaminophen-induced hepatic necrosis. I. Role of drug metabolism. *J Pharmacol Exp Ther*. **1973**, *187*, 185-194.

(42) Mitchell, J.R.; Thorgeirsson, S.S.; Potter, W.Z.; Jollow, D.J.; Keiser, H. Acetaminophen-induced hepatic injury: protective role of glutathione in man and rationale for therapy. *Clin Pharmacol Ther.* **1974**, *16*, 676-684.

(43) Griesbacher, T.; Amann, R.; Sametz, W.; Diethart, S.; Juan, H. The nonpeptide B2 receptor antagonist FR173657: inhibition of effects of bradykinin related to its role in nociception. *Br J Pharmacol*. **1998**, *124*, 1328–1334.

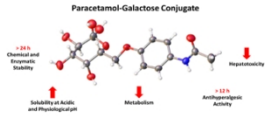

338x190mm (96 x 96 DPI)